catalysts

MDPI

Article

Novel Fe-W-Ce Mixed Oxide for the Selective Catalytic Reduction of NO_x with NH_3 at Low Temperatures

Anna Stahl [1,2,†], Zhong Wang [1,*,†], Tobias Schwämmle [2], Jun Ke [3] and Xuebing Li [1,*]

1 Key Laboratory of Biofuels, Qingdao Institute of Bioenergy and Bioprocess Technology, Chinese Academy of Sciences, Qingdao 266101, China; anna.lelickens@web.de
2 Institute of Combustion and Power Plant Technology, University of Stuttgart, Stuttgart 70569, Germany; tobias.schwaemmle@ifk.uni-stuttgart.de
3 School of Chemistry and Environmental Engineering, Wuhan Institute of Technology, Wuhan 430205, China; kejun1217@gmail.com
* Correspondence: wangzhong@qibebt.ac.cn (Z.W.), lixb@qibebt.ac.cn (X.L.); Tel./Fax: +86-532-8066-2757 (Z.W.); +86-532-8066-2759 (X.L.)
† These authors contributed equally to this work.

Academic Editors: Shaobin Wang and Xiaoguang Duan
Received: 16 January 2017; Accepted: 16 February 2017; Published: 20 February 2017

Abstract: A set of novel iron doped cerium-tungsten catalysts were prepared by sol-gel method with a view to their application for low temperature selective catalytic reduction (SCR) of NO_x with NH_3 in power plants. With a molar ratio Fe/W/Ce of 0.5:1:1, a NO_x reduction of >90% at 200 °C was achieved. In Fe-W-Ce catalysts with low iron oxide content, it was found that the iron compounds were highly dispersed and formed a solid solution within the cerium oxide lattice, which promoted the SCR activity. Large amounts of iron in the catalysts might form a layer of Fe_2O_3 on the catalyst surface, which induced the synergistic inhibition effect among Fe, Ce and W species. Moreover, the Fe-W-Ce catalysts possessed a high resistance to changed operation parameters as well as to deactivation by SO_2 and/or H_2O. The novel catalyst showed to be competitive among recently developed low-temperature SCR catalysts.

Keywords: Fe-W-Ce; SCR; synergistic effect; high resistance; competitive

1. Introduction

During combustion processes, many different kinds of pollutants can be generated, such as NO_x. NO_x emissions can have a strong negative impact on the environment and on human health, which result in photochemical smog and acid rain [1]. To avoid these damages, several techniques for the abatement of NO_x ($DeNO_x$) have been developed in the past. A widely applied technique of NO_x abatement is the selective catalytic reduction (SCR) with ammonia (NH_3) as reduction agent. Mostly vanadium catalysts on titanium support doped with tungsten or molybdenum oxide are commercially used (denoted as V_2O_5-WO_3/TiO_2 and V_2O_5-MoO_3/TiO_2, respectively) in a relatively narrow temperature window of 300–400 °C [2,3]. However this system has some problems, such as the volatility and toxicity of vanadium species, poisoning by K_2O and PbO, low N_2 selectivity at high temperatures and high conversion of SO_2 to SO_3 [4]. Therefore, it is necessary to develop novel catalysts that operate at lower temperatures [5].

With the aim to find a replacement for conventional catalysts, diverse catalysts have been studied extensively over the past years, such as Mn-oxides [6] and other transition metals oxides such as Ce-Fe/TiO_2 [7], CuO/$Ti_{0.95}Ce_{0.05}O_2$ [8], Ce-Nb binary oxide [9], Ba/CeO_2-MO_x (M = Mn, Fe) mixed oxides [10], Ce-Sn-O_x [11] or Ce-Ta mixed oxides [12] have been used as additives. Iron oxide

is reported to especially enhance the NO_x conversion at low temperatures. Moreover, Fe-doped Mn-Ce/TiO_2 catalysts can be used since iron is said to enhance the resistance to H_2O and SO_2 [13,14]. Additionally, the shift between Ce^{3+} and Ce^{4+} is also hold responsible for the enhancement of NO to NO_2 oxidation by cerium oxide, which favors the fast SCR reaction [15,16]. In addition, tungsten oxide is reported to widen the operation temperature window. For example, Shan et al. describe a NO_x conversion of almost 100% from 250 to 450 °C over Ce-W mixed oxides [17,18]. The WO_3-ZrO_2 catalyst exhibited >80% NO_x conversion at temperatures as low as 150 °C [19]. A reason may be that WO_3 is said to increase the strength and amount of Brönsted acid sites on catalyst surface [20]. Chen et al. assume that tungsten promotes the NO to NO_2 oxidation, which facilitates the fast SCR reaction that can occur at low temperatures [21]. Furthermore, tungsten seems to have the ability to inhibit the oxidation of NH_3 to N_2O and therefore increases the N_2 selectivity [19]. Besides, in combination with Ce, tungsten addition can lead to an improved dispersion of Ce and the amount of Ce^{3+} which leads to an increased chemisorption of oxygen [20].

Thus the combination of cerium and tungsten with iron might promise a high NO_x reduction ability at lower temperatures with a high N_2 selectivity and good resistance to deactivation by diverse compounds. This novel catalyst is developed and characterized, and the catalytic performance is also tested under diverse conditions, such as varying gas hourly space velocities (GHSV), SO_2 and H_2O flue gas content and NH_3/NO ratio. The results of these tests shall facilitate an estimation of the catalyst's behavior under "real" conditions in a power plant.

2. Results

2.1. Activity Measurement

Figure 1 shows the NH_3-SCR performance for all tested catalysts over a temperature range of 100 to 500 °C. Without Fe doping, the W-Ce catalyst showed more than 80% NO_x conversion at above 190 °C. The addition of Fe to W-Ce mixed oxide has obvious influence on the catalytic activity. When the Fe/W/Ce molar ratio was controlled at 0.5:1:1, the low temperature SCR activity was significantly enhanced with 80% NO_x conversion at 160 °C. Further increasing the Fe/W/Ce molar ratio to 1:1:1 and 2:1:1 resulted in the lower SCR activity, and the 80% NO_x conversion could be obtained at as high as 250 °C. Moreover, all catalysts also showed the higher N_2 selectivity (>95%) in the whole temperature range (Figure 1B). Therefore, the optimal Fe addition could contribute to improving the NH_3-SCR activity.

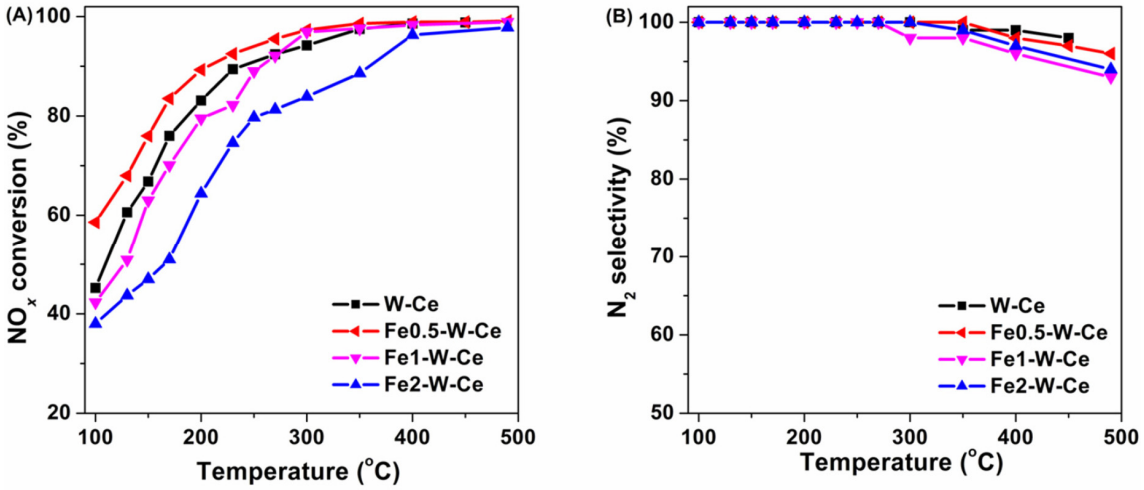

Figure 1. (**A**) NO_x conversion; and (**B**) N_2 selectivity of Fe-W-Ce catalysts. Reaction conditions: [NO_x] = 450 ppm, [NH_3] = 450 ppm, 2.5% O_2, N_2 as balance, GHSV = 20,000 h^{-1}.

2.2. BET and XRD

All the samples show type IV isotherms according to the International Union of Pure and Applied Chemistry (IUPAC) classification (shown in Figure S1), which are typical for mesoporous materials (pore diameter 2–50 nm) [8]. The results of the BET analysis for this study are listed in Table 1. It could be found that compared to W-Ce catalyst, the specific surface area was almost tripled at the highest iron loading. This also indicated that there was no link between a large specific surface area and a good catalytic performance. In addition, the molar ratio of Fe/W/Ce in samples (determined by inductively coupled plasma and atomic emission spectrometry (ICP-AES), Table 1) is more or less the same to the theoretical value. The XRD patterns of the Fe containing catalysts are compared to the W-Ce catalyst in Figure 2. All peaks of W-Ce catalyst can be assigned to cerianite (CeO_2, 2θ = 28.7°, 33.8°, 47.4°, 56.0°, 69.5° and 76.6°) and tungsten oxide (WO_3, 2θ = 23.7°, 28.7°, 33.8° 41.6°, 47.4°, 49.9°, 53.8° and 60.2°). This accorded with other studies in which CeO_2 and WO_3 were also the dominant species [21]. Meanwhile, the peaks were not very sharp, which pointed at low crystallinity of the sample [16]. This phenomenon might result from the addition of WO_3 to CeO_2 as reported in literature, which was regarded to be an indication of strong interactions between the metal oxides [22]. For Fe0.5-W-Ce catalyst, no new peaks appear, but the CeO_2 and WO_3 peaks became less intense and broader. This was reflected by the small crystallite size of the sample, which was usually associated with a high catalytic performance [22]. In addition, two possible explanations were given for the absence of new peaks from Fe compounds in Fe0.5-W-Ce. First, Fe oxides existed in an amorphous state and were highly dispersed over the surface of the WO_3 and CeO_2 lattice [14]. Second, smaller Fe ions (atomic radius 140 pm) can substitute larger Ce ions (atomic radius 185 pm) in the CeO_2 lattice [23], Fe/Ti oxides [24] as well as Fe/Mn oxides [25].

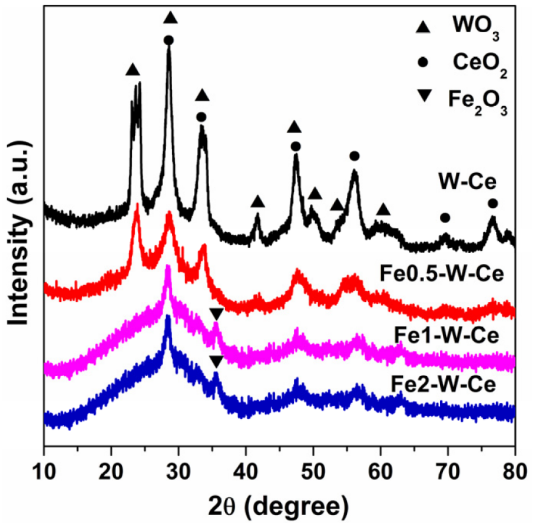

Figure 2. XRD patterns of Fe-W-Ce catalysts.

Table 1. Specific surface area and crystallite of different catalysts.

Samples	BET Surface Area (m^2/g)	Crystallite Size (nm)	Fe/W/Ce Molar Ratio [a]
W-Ce	24.8	10.5	1.09:0.96
Fe0.5-W-Ce	39.4	5.4	0.61:1.03:1.06
Fe1-W-Ce	53.2	7.3	1.08:0.95:1.03
Fe2-W-Ce	77.0	12.8	2.12:1.03:1.10

[a] Detected by ICP-AES.

For Fe1-W-Ce and Fe2-W-Ce catalysts, the larger crystallite size was observed compared with W-Ce and Fe0.5-W-Ce samples (Table 1). Nevertheless the peak at 35° allowed a clear identification as γ-Fe_2O_3, which has previously been reported to form in Fe catalysts [13]. Probably, the appearance of the peak meant that the Fe ions can no longer be incorporated into the Ce lattice. Instead, a layer of Fe_2O_3 formed on the catalyst surface. This phenomenon already occurred for other catalysts with high iron loadings [26]. It might be concluded that this Fe_2O_3 layer covered the catalyst surface and hindered the interaction between the W-Ce, which induced the lower NH_3-SCR activity.

2.3. Raman Characterization

Figure 3 depicts the Raman spectrum of the samples investigated in this work. The spectrum of W-Ce shows a sharp peak at 460 cm^{-1}, which belongs to the F_{2g} mode of the symmetric breathing mode of oxygen atoms surrounding cerium ions in the cubic fluorite phase CeO_2 [27]. In addition, typical WO_3 crystallization peaks (272, 711, and 810 cm^{-1}) occur on the W-Ce catalysts, which agrees with the XRD results. However, it is worth mentioning that the peak that belonged to the CeO_2 becomes weaker significantly for Fe0.5-W-Ce catalyst, which may be related with the decreased CeO_2 particle size (Table 1) [28]. As for Fe1-W-Ce and Fe2-W-Ce catalyst, the spectrum of CeO_2 becomes stronger than that of Fe0.5-W-Ce, suggesting that only proper adding of Fe inhibited the crystallization of CeO_2. The conclusion is highly consistent with the XRD results.

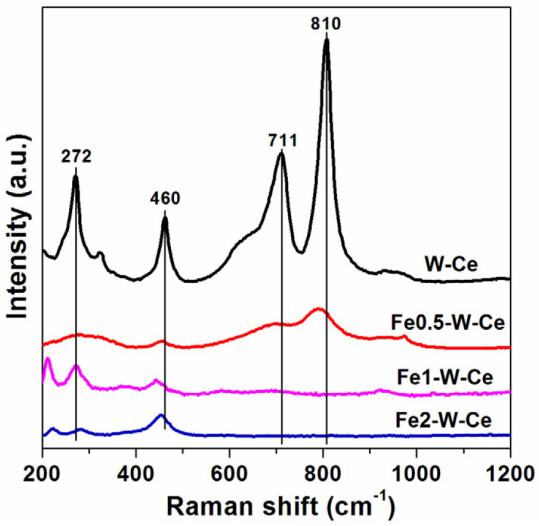

Figure 3. Raman patterns of Fe-W-Ce catalysts.

2.4. UV-Vis Diffuse Reflectance Spectroscopy

Figure 4 shows the UV-vis absorption spectra of W-Ce, Fe0.5-W-Ce, Fe1-W-Ce and Fe2-W-Ce. All samples contain three absorption maxima centered at ~230 nm, 290 nm and 320 nm. The former maxima corresponded to $Ce^{3+} \rightarrow O^{2-}$ charge transfer transitions [29], which implied the occurrence of oxygen vacancy defects [30]. The latter two adsorption maxima were ascribed to oxygen-to-Ce^{4+} charge transfer and interband transitions, respectively [31]. In addition, an additional peak shoulder can be identified around 380 nm, which is attributed to WO_3 [32]. An obvious blue shift of the peaks corresponding to tungsten and ceria compounds can be seen compared with pure WO_3. This may be a result of a strong interaction between tungsten and ceria species [33]. These findings are in accordance with the XRD results, which predicted also strong interaction between ceria and tungsten.

Meanwhile, Fe compounds show a broad peak centered at 530 nm. In literature the peak has been assigned to large Fe_2O_3 particles [34]. The intensity of the peaks can be correlated with the degree of dispersion of metal oxides. The Fe1-W-Ce catalyst shows a higher intensity peak of Fe_2O_3, suggesting that a relatively lower dispersion of Fe_2O_3 in Fe1-W-Ce catalyst. The peak intensity of

Fe2-W-Ce is higher than Fe1-W-Ce, which approves that Fe2-W-Ce shows the lowest dispersion of Fe_2O_3. The results confirm that the Fe compounds in Fe0.5-W-Ce are highly dispersed [24]. Overall, the UV-vis results are in full agreement with the conclusions drawn from the XRD. This includes the strong interaction between CeO_2 and WO_3, the high degree of iron dispersion in Fe0.5-W-Ce and the occurrence of large amounts of Fe_2O_3 in the Fe1-W-Ce and Fe2-W-Ce catalyst.

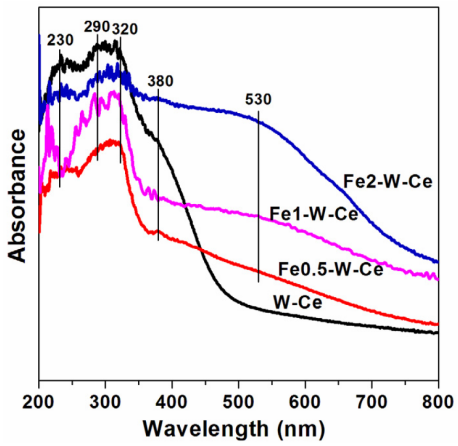

Figure 4. UV-vis of different catalysts.

2.5. Influence of GHSV and NH_3/NO Ratio

The NO_x reduction with different NH_3/NO ratios is shown in Figure 5. Previous experiments have been carried out with a NH_3/NO ratio of 1.2:1. The plot shows that there is a significant decrease of the overall NO_x reduction with a NH_3/NO ratio of 0.9:1. A maximal NO_x conversion of 91% is reached at 350 °C. Furthermore, the NO_x conversion decreases at temperatures >400 °C on NH_3/NO ratio of 0.9:1. This is not observed with higher NH_3/NO ratios. The NH_3/NO ratio has a strong influence on the NO_x conversion when it drops below the stoichiometric value of 1. In literature the SCR reaction is described to proceed with zero order concerning NH_3 at NH_3/NO > 1 and with first order for NH_3/NO < 1 [35]. This fits with the results shown in Figure 5. For NH_3/NO > 1 the adsorption process of NH_3 to the catalyst surface is said to limit the reaction progress [36]. This is reflected by the minimal difference of the results for NH_3/NO 1.1 and 1.2. The strong dependence is not seen as an obstacle for practical application, since the NH_3/NO ratio can be adapted while the process is running.

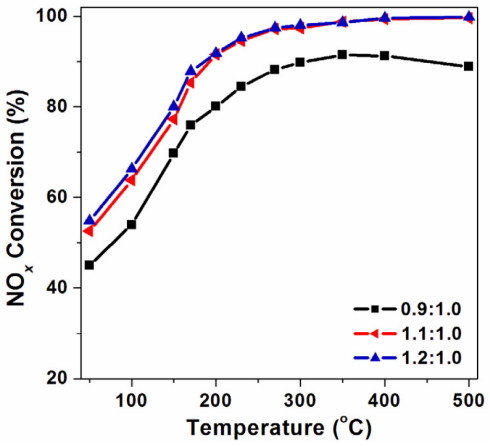

Figure 5. Influence of different NH_3/NO ratios on NO_x conversion over Fe0.5-W-Ce catalyst. Reaction conditions: [NH_3] = 450 ppm, 2.5% O_2, N_2 as balance, GHSV = 20,000 h^{-1}.

The influence of GHSV on NO_x reduction is tested. Figure 6 shows the slight decrease of NO_x conversion from 99% to 96% at 500 °C, when the GHSV is doubled from 20,000 to 40,000 h^{-1}. The GHSV has a less pronounced influence on the NO_x conversion compared to the NH_3/NO ratio. A variation of the GHSV of 50% (20,000 to 40,000 h^{-1}) leads to a NO_x conversion of 96%, while a change of the NH_3/NO ratio by only 25% (1.2 to 0.9) decreases the NO_x conversion to 91%. Hence, the SCR reaction is more sensitive to changes in the NH_3/NO ratio.

From Figure 6, it can be seen that the impact of GHSV also depends on the reaction temperature. At 500 °C the difference between the NO_x conversion with high and low GHSV is only 3.2%, while at lower temperatures, e.g., 170 °C, the difference is 13.1%. This connection was also found by other researchers [37]. The temperature dependence is problematic as far as the practical application is concerned, since it is intended to use the catalysts for low-temperature SCR.

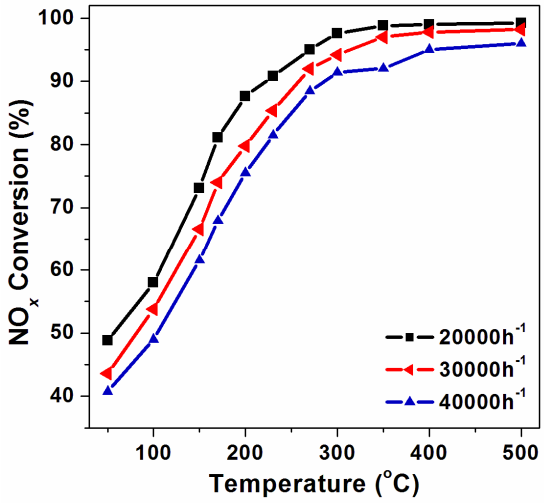

Figure 6. Influence of GHSV variation on NO_x conversion over Fe0.5-W-Ce catalyst. Reaction conditions: [NO_x] = 450 ppm, [NH_3] = 450 ppm, 2.5% O_2, N_2 as balance.

2.6. Influence of SO_2 and H_2O

The influence of additional gas streams of 200 ppm SO_2 and/or 5% H_2O on NO_x reduction is investigated. The temperature is kept constant at 350 °C. The NO_x reduction is registered some minutes before and after the additional gas streams are turned on and off. The results are displayed in Figure 7. After SO_2 addition, the NO_x conversion decreases from 99% to 95%. When water is added, the NO_x reduction decreases to 91% and when SO_2 and water are added simultaneously, it becomes about 84%. Furthermore, it is observed that the fluctuations of the measured NO_x concentrations increase in the following order: SO_2 < H_2O < SO_2 and H_2O. After the additional gases are turned off, the NO_x reduction efficiency returns in all three cases to a value very similar to the initial value.

The SO_2 and H_2O resistance of the Fe0.5-W-Ce catalyst is cross compared to some experimental values found in literature. The applied operation conditions vary widely. Especially the reaction temperature is reported to have a strong influence. At higher temperatures the impact of SO_2 and H_2O is less severe than at lower temperatures [38]. As mentioned above the SCR performance of the Fe0.5-W-Ce catalyst is investigated only at 350 °C. Other temperatures should be tested in future experiments. It is often stated that the influence of H_2O is reversible, while the impact of SO_2 on the reaction is permanent and only partial recovery is possible [39]. Therefore the terms "H_2O inhibition" and "SO_2 deactivation" are used. This strong influence is not observed in the present study. The NO_x conversion decrease is almost 100% reversible after H_2O and/or SO_2 treatment (Figure 7). Reasons for the good deactivation resistance can be found in the literature. Tungsten [19] and iron [14] are said to enhance the resistance of catalysts. For tungsten oxide, this fact is attributed to its ability to lower the thermal stability of cerium sulfates, which would otherwise block the active sites of the catalyst [21].

Since tungsten and iron are present in Fe0.5-W-Ce, it is assumed that in the current study these effects come into operation. Thus, the Fe0.5-W-Ce catalyst shows a very good resistance to SO_2 and H_2O poisoning, which supports its applicability in a power plant.

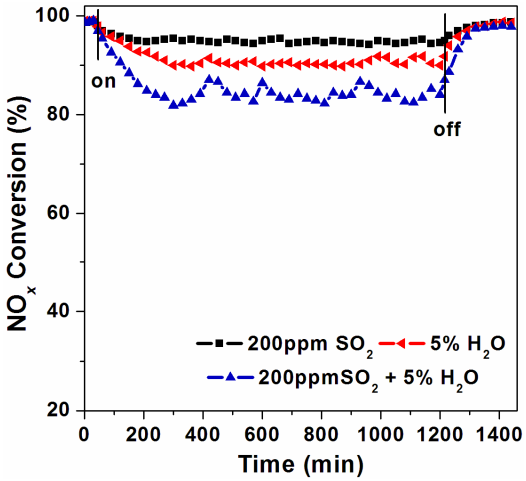

Figure 7. Influence of H_2O and/or SO_2 on NO_x conversion over Fe0.5-W-Ce catalyst. Reaction conditions: [NO_x] = 450 ppm, [NH_3] = 450 ppm, 2.5% O_2, N_2 as balance, GHSV = 20,000 h^{-1}.

In the stability test, the SCR reaction showed a stable behavior over 80 h (Figure 8). During the whole period, the NO_x reduction stays almost constant. It fluctuates between 99.0% and 98.4% with an average of 98.7%. Even though the Fe0.5-W-Ce catalyst shows a very good stability, the desired catalyst lifetime in practical application is thousands of hours-a timespan that can not be tested in laboratory scale experiments. Some researchers predict the deactivation of SCR catalysts by ammonium nitrate (NH_4NO_3) [40]. In the present experiment heating of the gas tubes is applied to exclude liquid water from the reaction and avoid NH_4NO_3 formation. A physicochemical characterization of the spend catalysts could reveal if ammonium nitrate is nevertheless formed in significant amounts.

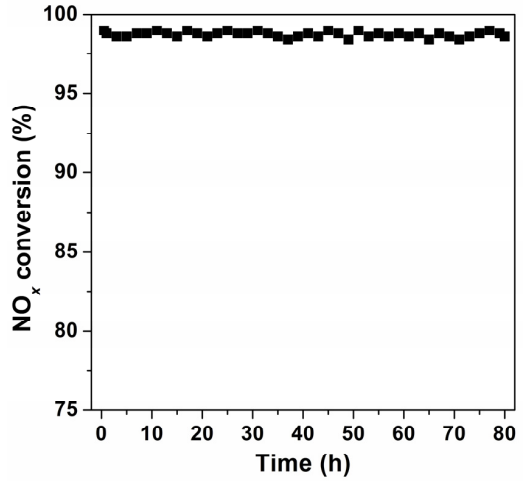

Figure 8. The long-term stability test on Fe0.5-W-Ce catalyst. Reaction conditions: [NO_x] = 450 ppm, [NH_3] = 450 ppm, 2.5% O_2, N_2 as balance, GHSV = 20,000 h^{-1}.

3. Discussion

It can be concluded that this Fe_2O_3 layer covers the catalyst surface and hinders the interaction between the CeO_2-WO_3 and the reactants in the gas phase (NO, NH_3). Hints to a highly dispersed form

of iron oxide in Fe0.5-W-Ce are given by the XRD, Raman and UV-vis results. The formation of a solid solution of Fe and Ce as a new active phase can lead to a higher NO_x reduction efficiency [25]. This can be an explanation why the Fe0.5-W-Ce performs better compared to the W-Ce catalyst. The idea that a large amount of Fe_2O_3 may cover the active sides of WO_x and CeO_2 in Fe1-W-Ce and Fe2-W-Ce is supported by the XRD and UV-vis results.

The XRD patterns of the samples after reaction are shown in Figure S2. The characteristic peaks of Fe-W-Ce catalysts are similar with that of the fresh samples (Figure 2), indicating the crystal structure of FeW-Ce are not destroyed after reaction. Furthermore, no significant changes for the characteristic peaks of Fe0.5-W-Ce after the experiments of SO_2 and H_2O resistance are observed (Figures S3 and S4), suggesting the Fe0.5-W-Ce could possess the high stability. Nevertheless, the catalyst after the experiments of SO_2 and H_2O resistance results in a decrease in surface area (Table S1). The decrease in BET surface area is primarily due to the surface sulfate species formation.

At the first glance, the weak SCR performance of Fe1-W-Ce and Fe2-W-Ce samples seem to be contradictory to its high specific surface area. However, as mentioned before, the direct neighbors of each atom in a crystal lattice are more important for the SCR than the overall crystallinity [21]. In the next step, the SCR performance of the novel catalysts shall be compared to previous studies. For this task, three criteria are chosen: the NO_x conversion, the lowest operation temperature, and the size of the operation temperature window. It is important to define the term "operation temperature" as it is used in this study. Two definitions for low temperature SCR applications exist in literature: some researchers claim that the operation temperature window comprises the temperature range where the NO_x reduction is >80% [41]. Other research groups set a threshold of >90% NO_x reduction [25]. Because stricter legal regulations for NO_x emissions can be expected in the future the value of 90% is used in this study. The lowest operation temperature should be in the ideal case <200 °C, since this is the temperature of the flue gases at the tail-end of a power plant.

Firstly, catalysts that contain only cerium and tungsten oxides shall be compared. Our W-Ce catalyst reaches the threshold of 90% NO_x reduction at 230 °C and slightly misses the ideal operation temperature of <200 °C. The maximum NO_x reduction for these catalysts is 99%. The catalysts of other research groups show a similarly high efficiency (Table 2). Peng et al. reached the 90% mark at 185 °C [42], Ma et al. at 190 °C [33], Shan et al. at 215 °C [17] and Liu et al. at 290 °C [43]. It has to be kept in mind that different preparation techniques and operation conditions have been used. Roughly speaking, the W-Ce catalyst achieves average performance results. Considering the iron oxide catalysts, Fe0.5-W-Ce achieves a NO_x reduction >90% at 200 °C and a maximal NO_x reduction of 99%. It therefore fulfills the criteria set for a low temperature SCR catalyst. In literature one finds iron oxide catalysts with >90% NO_x reduction at 150 °C [13] and at 350 °C [35]. Another Fe catalysts prepared by the sol-gel method only reaches 55% maximal NO_x reduction [14].

Table 2. Comparison of the activity for NH_3-SCR on different catalysts.

Samples	Reaction Conditions	Temperature (°C)	NO_x Conversion (%)	References
Fe_2O_3	500 ppm NO, 500 ppm NH_3, 3% O_2, and balance N_2	150	90	[13]
Fe-Mn-Ce/TiO_2	0.06 vol % NO, 0.06 vol % NH_3, 3 vol % O_2 and pure N_2 in balance	180	96	[14]
Ce-W	500 ppm NO, 500 ppm NH_3, 5 vol % O_2, balance N_2	215	90	[17]
WO_3/CeO_2	500 ppm NO, 500 ppm NH_3, 5% O_2 and N_2 in balance	190	90	[33]
Co/Fe_2O_3	[NO] = 500 ppm, [NH_3] = 500 ppm, [O_2] = 2 vol %, balance gas: N_2	350	90	[35]
Mn-CeO_2-WO_3	0.05% NO, 0.05% NH_3, 3% O_2, and in a N_2 stream.	185	90	[42]
CeO_2-WO_3	500 ppm NO, 500 ppm NH_3, 3 vol % O_2 and balance in N_2	290	90	[43]

4. Materials and Methods

4.1. Catalyst Preparation

Four W-Ce catalysts doped with different amounts of Fe were prepared by the sol-gel method. First an appropriate amount of ammonium tungstate was added to deionized water under continuous stirring. To dissolve the ammonium tungstate, an equal amount of oxalic acid dihydrate was added and the solution was mixed until it became clear. The molar ratios were Fe/W/Ce = 0:1:1, 0.5:1:1, 1:1:1 and 2:1:1. The $Fe(NO_3)_3 \cdot 9H_2O$ and $Ce(NO_3)_3 \cdot 6H_2O$ was the source of iron and Cerium, respectively. As complexing agent citric acid was added in a molar ratio of 1.3:1 to all metal ions. Last polyethylene glycol (PEG) was added in an amount corresponding to 50% (*w*/*w*) of citric acid. Afterwards, the samples were heated to 80 °C under ongoing stirring until the gel formation was completed. The gel was then put to a furnace at 120 °C until the gel was dry. Subsequently, the samples were calcined at 500 °C for 3 h. After calcination, the catalysts were pressed, crushed and sieved to 20–40 mesh. The catalysts are denoted as Fe*x*-W-Ce, and *x* stands for the molar ratio of Fe to W.

4.2. Catalyst Characterization

The specific surface areas were obtained from N_2 adsorption/desorption isotherms measured on a Micromeritics ASAP 2020 M (Quantachrome, Boynton Beach, FL, USA) at −196 °C, then are calculated using the Brunauer–Emmett–Teller (BET) method. The ICP-AES was used to determine the molar ratio of Fe/W/Ce in the synthesized samples, which was performed on an OPTIMA 2000 (PerkinElmer, Waltham, MA, USA). The XRD patterns of catalysts were collected on a Bruker AXS-D8 Advance powder diffractometer (Bruker, Karlsruhe, Germany) with a Cu Kα radiation source of wavelength 1.5406 Å, and the crystallite size was calculated by the main peak at 28.7° according to Scherrer's equation. UV Raman spectra were recorded on a DXR Microscope Raman spectrograph (ThermoFisher Scientific, Waltham, MA, USA) with He-Cd laser of 325 nm excitation wavelength. The UV-vis diffuse reflectance spectroscopy (DRS) was carried out on a Hitachi U-4100 UV/Vis/NIR spectrophotometer (Hitachi, Tokyo, Japan), and wavelengths from 200 to 800 nm were scanned for light absorption.

4.3. Activity Measurement

The NH_3-SCR activity was performed in a fixed bed reactor using a MRU vario plus industrial flue gas measurement device. The Fe-W-Ce catalyst (0.3 g, 20–40 mesh) was mixed with silica sand (0.4 g, 20–40 mesh), and then filled into a quartz reactor with 8 mm inner diameter. The reaction conditions were controlled as follows: 450–500 ppm NO_x, 450–500 ppm NH_3, 2.5% O_2, N_2 as balance. Before the activity test, the measured values of the gas concentrations were allowed to stabilize at room temperature for around 1.5 h. Each temperature was kept until the measured values stabilize (40–60 min).

5. Conclusions

The investigation of the SCR performance reveals a good NO_x conversion and high resistance to differences in operation parameters as well as to poisoning by flue gas compounds. In comparison to the literature, the very wide operation temperature window of the W-Ce and the Fe0.5-W-Ce catalyst is remarkable. A NO_x reduction of >90% is reached over a span of 260 °C for W-Ce and over a span of 290 °C for Fe0.5-W-Ce. This indicates that the newly developed catalysts can be used in low temperature SCR as well as at higher temperatures. They are very flexible in application.

Supplementary Materials: The following are available online at www.mdpi.com/2073-4344/7/2/71/s1, Figure S1: The N_2 adsorption-desorption isotherms of Fe-W-Ce catalysts, Figure S2: XRD patterns of Fe-W-Ce catalysts after reaction, Figure S3: XRD patterns of Fe0.5-W-Ce catalysts after reaction (a: SO_2 + NO_x + NH_3 + O_2, b: SO_2 + NO_x + NH_3 + H_2O + O_2), Figure S4: Raman patterns of Fe0.5-W-Ce catalysts after reaction (a: SO_2 + NO_x + NH_3 + O_2, b: SO_2 + NO_x + NH_3 + H_2O + O_2), Table S1: Specific surface area and crystallite size of Fe0.5-W-Ce catalysts after reaction.

Acknowledgments: The work described above was supported by the National Natural Science Foundation of China (No: 21607162, 21276263 and 21506239), the Doctoral Fund of Shandong Province (BS2015HZ003), Qingdao Indigenous Innovation Program (16-5-1-27-jch) and the Open Foundation of Key Laboratory of Industrial Ecology and Environmental Engineering, MOE (KLIEEE-15-05).

Author Contributions: Zhong Wang and Xuebing Li conceived and designed the experiments; Anna Stahl performed the experiments; Anna Stahl and Zhong Wang analyzed the data; Anna Stahl and Zhong Wang wrote the paper; and Jun Ke and Tobias Schwämmle revised the paper.

Conflicts of Interest: The authors declare no conflict of interest.

References

1. Parvulescu, V.; Grange, P.; Delmon, B. Catalytic removal of NO. *Catal. Today* **1998**, *46*, 233–316. [CrossRef]
2. Qi, G.; Yang, R. Low-temperature selective catalytic reduction of NO with NH_3 over iron and manganese oxides supported on titania. *Appl. Catal. B* **2003**, *44*, 217–225. [CrossRef]
3. Alemany, J.; Lietti, L.; Ferlazzo, N.; Forzatti, P.; Busca, G.; Ramis, G.; Giamello, E.; Bregani, F. Reactivity and physicochemical characterisation of V_2O_5-WO_3/TiO_2 De-NO_x catalysts. *J. Catal.* **1995**, *155*, 117–130. [CrossRef]
4. Kamata, H.; Takahashi, K.; Odenbrand, C. The role of K_2O in the selective reduction of NO with NH_3 over a $V_2O_5(WO_3)/TiO_2$ commercial selective catalytic reduction catalyst. *J. Mol. Catal. A* **1999**, *139*, 189–198. [CrossRef]
5. Lee, S.; Park, K.; Kim, S.; Kwon, D.; Hong, S. Effect of the Mn oxidation state and lattice oxygen in Mn-based TiO_2 catalysts on the low-temperature selective catalytic reduction of NO by NH_3. *J. Air Waste Manag. Assoc.* **2012**, *62*, 1085–1092. [CrossRef] [PubMed]
6. Eigenmann, F.; Maciejewski, M.; Baiker, A. Selective reduction of NO by NH_3 over manganese-cerium mixed oxides: Relation between adsorption, redox and catalytic behavior. *Appl. Catal. B* **2006**, *62*, 311–318. [CrossRef]
7. Shu, Y.; Tanana, A.; Quan, X.; Chen, S.; Yu, H.T. Selective catalytic reaction of NO_x with NH_3 over Ce-Fe/TiO_2-loaded wire-mesh honeycomb: Resistance to SO_2 poisoning. *Appl. Catal. B* **2014**, *150–151*, 630–635. [CrossRef]
8. Guo, R.T.; Zhen, W.L.; Pan, W.G.; Zhou, Y.; Hong, J.N.; Xu, H.J.; Jin, Q.; Ding, C.G.; Guo, S.Y. Effect of Cu doping on the SCR activity of CeO_2 catalyst prepared by citric acid method. *J. Ind. Eng. Chem.* **2014**, *20*, 1577–1580. [CrossRef]
9. Qu, R.; Gao, X.; Cen, K.; Li, J. Relationship between structure and performance of a novel cerium-niobium binary oxide catalyst for selective catalytic reduction of NO with NH_3. *Appl. Catal. B* **2013**, *142–143*, 290–297. [CrossRef]
10. Mousavi, S.; Niaei, A.; Gómez, M.; Salari, D.; Panahi, P.; Abaladejo-Fuentes, V. Characterization and activity of alkaline earth metals loaded CeO_2-MO_x (M = Mn, Fe) mixed oxides in catalytic reduction of NO. *Mater. Chem. Phys.* **2014**, *3*, 921–928. [CrossRef]
11. Li, X.; Li, Y.; Deng, S.; Rong, T. A Ce-Sn-O_x catalyst for the selective catalytic reduction of NO_x with NH_3. *Catal. Commun.* **2013**, *40*, 47–50. [CrossRef]
12. Zhang, T.; Qu, R.; Su, W.; Li, J. A novel Ce-Ta mixed oxide catalyst for the selective catalytic reduction of NO_x with NH_3. *Appl. Catal. B* **2015**, *176–177*, 338–346. [CrossRef]
13. Wang, X.; Gui, K. Fe_2O_3 particles as superior catalysts for low temperature selective catalytic reduction of NO with NH_3. *J. Environ. Sci.* **2013**, *12*, 2469–2475. [CrossRef]
14. Shen, B.; Liu, T.; Zhao, N.; Yang, X.; Deng, L. Iron-doped Mn-Ce/TiO_2 catalyst for low temperature selective catalytic reduction of NO with NH_3. *J. Environ. Sci.* **2010**, *9*, 1447–1454. [CrossRef]
15. Liu, C.; Chen, L.; Li, J.; Ma, L.; Arandiyan, H.; Du, Y.; Xu, J.; Hao, J. Enhancement of activity and sulfur resistance of CeO_2 supported on TiO_2-SiO_2 for the selective catalytic reduction of NO by NH_3. *Environ. Sci. Technol.* **2012**, *11*, 6182–6189. [CrossRef] [PubMed]
16. Liu, J.; Li, Y.; Ke, J.; Wang, Z.; Xiao, H.N. Synergically improving light harvesting and charge transportation of TiO_2 nanobelts by deposition of MoS_2 for enhanced photocatalytic removal of Cr(VI). *Catalysts* **2017**, *7*, 30. [CrossRef]
17. Shan, W.; Liu, F.; He, H.; Shi, X.; Zhang, C. Novel cerium-tungsten mixed oxide catalyst for the selective catalytic reduction of NO_x with NH_3. *Chem. Commun.* **2011**, *47*, 8046–8048. [CrossRef] [PubMed]

18. Nie, J.; Wu, X.; Ma, Z.; Xu, T.; Si, Z.; Chen, L.; Weng, D. Tailored temperature window of MnO_x-CeO_2 SCR catalyst by addition of acidic metal oxides. *Chin. J. Catal.* **2014**, *35*, 1281–1288. [CrossRef]
19. Kwon, D.; Nam, K.; Hong, S. Influence of tungsten on the activity of a Mn/Ce/W/Ti catalyst for the selective catalytic reduction of NO with NH_3 at low temperatures. *Appl. Catal. A* **2015**, *497*, 160–166. [CrossRef]
20. Jiang, Y.; Xing, Z.; Wang, X.; Huang, S.; Wang, X.; Liu, Q. Activity and characterization of a Ce-W-Ti oxide catalyst prepared by a single step sol-gel method for selective catalytic reduction of NO with NH_3. *Fuel* **2015**, *151*, 124–129. [CrossRef]
21. Li, P.; Xin, Y.; Li, Q.; Wang, Z.; Zhang, Z.; Zheng, L. Ce-Ti amorphous oxides for selective catalytic reduction of NO with NH_3: Confirmation of Ce-O-Ti active sites. *Environ. Sci. Technol.* **2012**, *17*, 9600–9605. [CrossRef] [PubMed]
22. Ke, J.; Liu, J.; Sun, H.Q.; Zhang, H.Y.; Duan, X.G.; Liang, P.; Li, X.Y.; Moses, O.T.; Liu, S.M.; Wang, S.B. Facile assembly of Bi_2O_3/Bi_2S_3/MoS_2 *n-p* heterojunction with layered *n*-Bi_2O_3 and *p*-MoS_2 for enhanced photocatalytic water oxidation and pollutant degradation. *Appl. Catal. B* **2017**, *200*, 47–55. [CrossRef]
23. Xing, W.; Qian, K.; Dao, L. Catalytic combustion of chlorobenzene over MnO_x-CeO_2 mixed oxide catalysts. *Appl. Catal. B* **2009**, *86*, 166–175. [CrossRef]
24. Liu, F.; He, H.; Zhang, C.; Feng, Z.; Zheng, L.; Xie, Y.; Hu, T. Selective catalytic reduction of NO with NH_3 over iron titanate catalyst: Catalytic performance and characterization. *Appl. Catal. B* **2010**, *96*, 408–420. [CrossRef]
25. Liu, F.; He, H.; Ding, Y.; Zhang, C. Effect of manganese substitution on the structure and activity of iron titanate catalyst for the selective catalytic reduction of NO with NH_3. *Appl. Catal. B* **2009**, *93*, 194–204. [CrossRef]
26. Peña, D.; Uphade, B.; Smirniotis, P. TiO_2-supported metal oxide catalysts for low-temperature selective catalytic reduction of NO with NH_3. I. Evaluation and characterization of first row transition metals. *J. Catal.* **2004**, *221*, 421–431. [CrossRef]
27. Wang, Z.; Qu, Z.P.; Quan, X.; Wang, H. Selective catalytic oxidation of ammonia to nitrogen over ceria-zirconia mixed oxides. *Appl. Catal. A* **2012**, *411–412*, 131–138. [CrossRef]
28. Xu, J.; Li, P.; Song, X.; He, C.; Yu, J.; Han, Y. Operando Raman spectroscopy for determining the active phase in one-dimensional $Mn_{1-x}Ce_xO_{2\pm y}$ nanorod catalysts during methane combustion. *J. Phys. Chem. Lett.* **2010**, *1*, 1648–1654. [CrossRef]
29. Bensalem, A.; Verduraz, F.B.; Delamar, M.; Bugli, G. Preparation and characterization of highly dispersed silica-supported ceria. *Appl. Catal. A* **1995**, *121*, 81–93. [CrossRef]
30. Reddy, B.M.; Rao, K.N.; Bharali, P. Copper promoted cobalt and nickel catalysts supported on ceria-alumina mixed oxide: Structural characterization and CO oxidation activity. *Ind. Eng. Chem. Res.* **2009**, *48*, 8478–8486. [CrossRef]
31. Liu, L.; Yao, Z.; Deng, Y.; Gao, F.; Liu, B.; Dong, L. Morphology and crystal-plane effects of nanoscale ceria on the activity of CuO/CeO_2 for NO reduction by CO. *ChemCatChem* **2011**, *3*, 978–989. [CrossRef]
32. Si, Z.; Wu, X.; Weng, D.; Ma, Z.; Ma, J. Tailored temperature window of CuO_x/WO_x-ZrO_2 for NO_x reduction via adjusting the calcination temperature of WO_x-ZrO_2. *Mater. Chem. Phys.* **2013**, *138*, 399–404. [CrossRef]
33. Ma, Z.; Weng, D.; Wu, X.; Si, Z. Effects of WO_x modification on the activity, adsorption and redox properties of CeO_2 catalyst for NO_x reduction with ammonia. *J. Environ. Sci.* **2012**, *7*, 1305–1316. [CrossRef]
34. Hong, W.J.; Ueda, M.; Iwamoto, S.; Hosokawa, S.; Wada, K.; Kanai, H.; Deguchi, H.; Inoue, M. Effect of Fe content on physical properties of BaO-CeO_x-FeO_y catalysts for direct NO decomposition. *Appl. Catal. B* **2011**, *106*, 142–148. [CrossRef]
35. Wang, C.; Yang, S.; Chang, H.; Peng, Y.; Li, J. Structural effects of iron spinel oxides doped with Mn, Co, Ni and Zn on selective catalytic reduction of NO with NH_3. *J. Mol. Catal. A* **2013**, *376*, 13–21. [CrossRef]
36. Yang, J.; Ma, H.; Yamamoto, Y.; Yu, J.; Xu, G.; Zhang, Z.; Suzuki, Y. SCR catalyst coated on low-cost monolith support for flue gas denitration of industrial furnaces. *Chem. Eng. J.* **2013**, *230*, 513–521. [CrossRef]
37. Chen, L.; Li, J.; Ge, M. Promotional effect of Ce-doped V_2O_5-WO_3/TiO_2 with low vanadium loadings for selective catalytic reduction of NO_x by NH_3. *J. Phys. Chem. C* **2009**, *113*, 21177–21184. [CrossRef]
38. Yu, M.; Li, C.; Zeng, G.; Zhou, Y.; Zhang, X.; Xie, Y. The selective catalytic reduction of NO with NH_3 over a novel Ce-Sn-Ti mixed oxides catalyst: Promotional effect of SnO_2. *Appl. Surf. Sci.* **2015**, *342*, 174–182. [CrossRef]

39. Lee, S.; Park, K.; Hong, S. MnO_x/CeO_2-TiO_2 mixed oxide catalysts for the selective catalytic reduction of NO with NH_3 at low temperature. *Chem. Eng. J.* **2012**, *195–196*, 323–331. [CrossRef]
40. Ma, Z.; Wu, X.; Feng, Y.; Si, Z.; Weng, D. Effects of WO_3 doping on stability and N_2O escape of MnO_x-CeO_2 mixed oxides as a low-temperature SCR catalyst. *Catal. Commun.* **2015**, *69*, 188–192. [CrossRef]
41. Chen, L.; Si, Z.; Wu, X.; Weng, D.; Ran, R.; Yu, J. Rare earth containing catalysts for selective catalytic reduction of NO_x with ammonia: A review. *J. Rare Earths* **2014**, *10*, 907–917. [CrossRef]
42. Peng, Y.; Liu, Z.; Niu, X.; Zhou, L.; Fu, C.; Zhang, H.; Li, J.; Han, W. Manganese doped CeO_2-WO_3 catalysts for the selective catalytic reduction of NO_x with NH_3: An experimental and theoretical study. *Catal. Commun.* **2012**, *19*, 127–131. [CrossRef]
43. Liu, C.; Chen, L.; Chang, H.; Ma, L.; Peng, Y.; Arandiyan, H.; Li, J. Characterization of CeO_2-WO_3 catalysts prepared by different methods for selective catalytic reduction of NO_x with NH_3. *Catal. Commun.* **2013**, *40*, 145–148. [CrossRef]

© 2017 by the authors. Licensee MDPI, Basel, Switzerland. This article is an open access article distributed under the terms and conditions of the Creative Commons Attribution (CC BY) license (http://creativecommons.org/licenses/by/4.0/).